Jomard Publishing

VIBRATIONAL AND X-RAY MEASUREMENTS OF La$_2$Ti$_2$O$_7$ UNDER HIGH PRESSURE CONDITION

iD **A.G. Asadov[1,2*], A.I. Mammadov[1], R.Z. Mehdiyeva[1],**
E.R. Huseynova[1], D.M. Mirzayeva[3]

[1]Institute of Physics, Azerbaijan National Academy of Sciences, Baku, Azerbaijan
[2]Frank Laboratory of Neutron Physics, JINR, Dubna, Russia
[3]Western Caspian University, Baku, Azerbaijan

Abstract. The present study focuses on investigating the impact of high-pressure conditions on the crystal structure and vibration spectra of the perovskite-like layered compound La$_2$Ti$_2$O$_7$. To this end, X-ray diffraction and Raman spectroscopy techniques were employed to observe the behavior of the compound under pressure levels up to 30 GPa. The neutron diffraction at ambient pressure confirms that the structure of La$_2$Ti$_2$O$_7$ is monoclinic P2$_1$. The results indicate that when the pressure attains 17.3 GPa, the original monoclinic phase of P2$_1$ symmetry undergoes a phase transition to the monoclinic phase of P2 symmetry. The observed pressure-induced phase transitions in La$_2$Ti$_2$O$_7$ are associated with anomalous changes in both the unit cell parameters and the vibrational modes. Additionally, the study obtained the baric dependences of lattice parameters, unit cell volume and vibration frequencies, which were used to calculate the bulk modules for the initial and pressure-induced phases of La$_2$Ti$_2$O$_7$.

1.   Introduction

Recently the popularity of rare-earth titanites is increasing due to their broad application areas in engineering and technology (Gao *et al*., 2017; Wang *et al*., 2010; López-Pérez & Íñiguez, 2011; Yan *et al*., 2009). Possession of strong piezoelectric and electro-optic characters make these materials valuable as a sensors and actuators in chemical and material processing, automotive and power generating industries (Yan *et al*., 2009; Nanamatsu *et al*., 1974). Structural stability highly depend on cation radii ratio of Ln^{3+} and Ti^{4+}. The radius of cations in A$_2$B$_2$O$_7$ composition family has three structural domination: fluorite (r_A/r_B < 1.48), pyrochlore (1.48 < r_A/r_B <1.78) and perovskite-like layered (PL) (r_A/r_B > 1.78) structure. Here Ln^{3+} is A site cation and Ti^{4+} is B site cation and these structures are complex (Gao *et al*., 2017; 2013; Wang *et al*., 2010; 2022; López-Pérez & Íñiguez, 2011; Hwang *et al*., 2003; Yamamoto *et al*., 1980; Nanamatsu *et al*., 1974). As a member of A$_n$B$_n$O$_{3n+2}$ (n=4) family Ln–Ti–O (Ln =La, Nd, Pr) ternary

systems are possess only PL structure (Sivagnanapalani *et al.*, 2021). Some perovskite compounds are characterized by their non-centrosymmetric crystal symmetry and monoclinic structure, where their respective space group is $P2_1$. The presence of a non-centrosymmetric crystal symmetry is a prerequisite for the ferroelectricity of these compounds, with transition temperatures of 1461, 1482 and 1750^0C for $La_2Ti_2O_7$, $Nd_2Ti_2O_7$ and $Pr_2Ti_2O_7$, respectively (Patwe *et al.*, 2015). PL structure is characterized with corner shared BO_6 octahedrons and 12-coordinated A cations thus perovskite like layers separated by oxygen rich gaps which are linked by A cations at their boundaries and this structure considered as a cutting the cubic perovskite ABO_3 structure along [110] direction followed by an insertion of additional oxygen (Gao *et al.*, 2017; Nanamatsu *et al.*, 1974; Sivagnanapalani *et al.*, 2021). The $La_2Ti_2O_7$ is translucent. Generally, $Ln_2Ti_2O_7$ (Ln = La, Nd, Pr) PL structures known as larger A/B ionic radius ratio (Gao *et al.*, 2017). For the ambient conditions LTO has been shown to have condition depended modifications as $P2_1$ monoclinic, $Cmc2_1$ orthorhombic, Cmcm orthorhombic, $Pna2_1$ orthorhombic (Yamamoto *et al.*, 1980). By the increasing of temperature structure turns to $Cmc2_1$ phase at 773K (Hwang *et al.*, 2003), till this point displacements of the La atoms take place within the respective planes perpendicular to the a-axis and by rotations of TiO_6 octahedra around an axis parallel to the b-axis and through the respective Ti atoms (Patwe *et al.*, 2015) and also when the temperature reach to 1773 K structure turns Cmcm orthorhombic with the observed shifting and tilting through crystal (López-Pérez & Íñiguez, 2011; Hwang *et al.*, 2003; Patwe *et al.*, 2015; Ishizawa *et al.*, 1982). In the complexity of LTO structure makes challenging to obtain full Rietveld refinement of all atomic coordinates at high pressures, especially for oxygen atoms. The reason is, there are 4 La ions, 4 Ti ions and 14 O anions in the unit cell (Z=2) and they all occupy 2a Wyckoff positions, thus it become overlapping of intensity peaks at high pressure (Gao *et al.*, 2013).

The impact of extreme conditions on the crystal structure of materials can have profound effects on their physical and chemical properties. Such extreme conditions may arise from exposure to radiation, variations in temperature or changes in pressure. Radiation, for instance, can lead to the formation of defects in crystals (Yan *et al.*, 2009), altering their electronic and mechanical properties (Mirzayev *et al.*, 2019) or even cause amorphisation and gain new thermodynamic properties (Mirzayev, 2020), where the crystalline structure is lost, leading to further changes in material properties. The study of these effects is critical for the development of new materials with tailored properties and for understanding the behavior of materials in high-stress environments, such as in nuclear reactors or in outer space. In order to figure out the behavior of crystal at high-pressure, the experiments below were set.

2. Materials and methods

2.1. Neutron diffraction

For the precise exploration and determination by high temperature and pressure range of research of magnetic and crystal structure of powder materials the neutron diffractometer DN-6 at the IBR-2 high-flux reactor is used for the studies of crystal and magnetic structure of powder materials. The high neutron flux on the sample due to a parabolic focusing section of a neutron guide and wide solid angle of the detector system enables neutron diffraction experiments with extraordinarily small volumes (0.01 mm^3) of studied samples (Kozlenko *et al.*, 2018). The studies of LTO at ambient condition

confirms the structure of LTO is monoclinic P2$_1$ (a = 7.75, b = 12.91, c = 5.51, β = 98.74, V = 545.1 Å^3) Z=2 with 22 atoms in unit cell (Mirzayev *et al.*, 2020), ligand Ti atoms surrounded by six O atoms and create TiO$_6$ octahedrons so slabs separated by La3, La4 atoms (Figure 1).
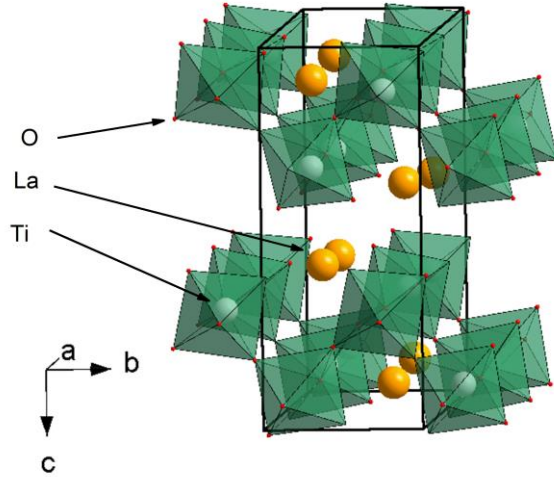

Figure 1. La$_2$Ti$_2$O$_7$ strucuture at ambient condition with P2$_1$ space group

Rietveld refinement for neutron diffraction refined with Fullprof software (Zhang *et al.*, 2007). The *d$_{hkl}$* interplanar distances for intensive peaks are shows that, structure has P2$_1$.
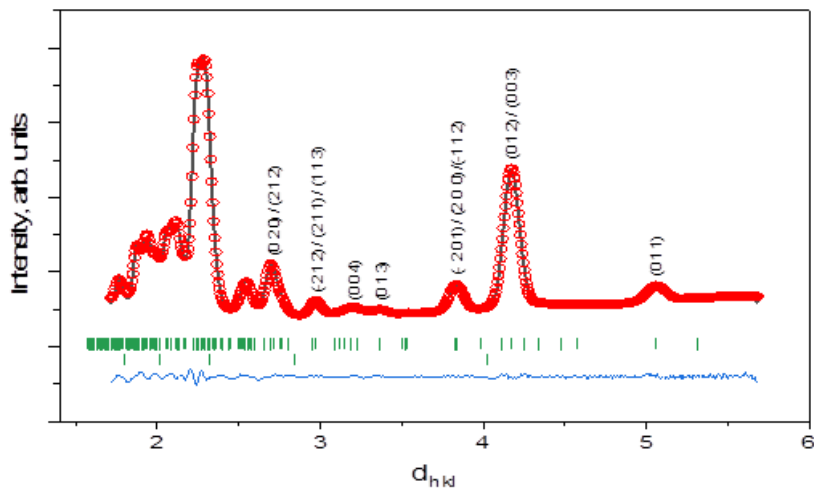

Figure 2. Neutron diffraction pattern of La$_2$Ti$_2$O$_7$. The selected peaks confirm monoclinic P2$_1$ structure of LTO at ambient conditions

It is clearly observed that LTO adopt the expected monoclinic (P2$_1$) structure (α-phase) with the (00l) orientations.

Table 1. d-Spacing values for different crystallographic planes of $La_2Ti_2O_7$

Plane	d-Spacing (Å)
011	5.05(8)
012/003	4.25(8)
200/-201	3.83(6)
013	3.36(7)
004	3.19(3)
211	2.96(9)
020/212	2.75(5)

2.2. X-ray diffraction

The XRD analysis was carried out using a Xeuss 3.0 diffractometer with a MoK source (wavelength $\lambda = 0.710781$ Å) and a diamond anvil cell (DAC) as a pressure inducer. The sample was placed between the DAC and a diamond with a drilled Re (rhenium) sample holder with a diameter 150 µm. The pressure was measured using the pressure dependence of the photoluminescent emission of Ruby balls (Al_2O_3) as a function of pressure (Schmalle *et al*., 1993), with LaB_6 used for calibration at the top of the DAC.The results of the XRD analysis showed continuous broadening and shifting of the pattern without interruption until reaching a pressure of 16.3 GPa. The high-pressure phase demonstrated a completely uncommon pattern from the low-pressure phase for the relative intensities of strong peaks. The low-pressure phase (up to 2.2 GPa) is very close to the XRD pattern of the initial materials, confirming that the pressure-induced phase transition is reversible. It is worth noting that the noticeable differences in the X-ray diffraction pattern of LTO from 1 atm to 16.3 GPa are not related to structural changes, but can be explained by the pressure effect on the crystal. The crystal unit cell parameters and diffraction peaks show anomalous effects for the monoclinic structure at 17.3 GPa and the tendecy followed up to 31.8 GPa. The Raman spectra also confirm that there are some changes between this interval.

Pressure induced X-ray diffraction at Figure 3 shows the effect of pressure on X-ray pattern. The X-ray diffraction data were analyzed by the FullProf software (Zhang *et al*., 2007). In order to figure out the high-pressure phase of $La_2Ti_2O_7$ we have considered to reported structural details for high temperature phase transition of monoclinic ($P2_1$) and orthorhombic (Cmcm and $Cmc2_1$) symmetries of $La_2Ti_2O_7$ (Alanis *et al*., 2019). Thus, the Rietveld refinements of the powder X-ray diffraction (XRD) were carried by considering all the possible models based on $La_2Ti_2O_7$ and related structure types, viz. $P2_1$, P2, $P2_1$/m. $Cmc2_1$ and Cmcm symmetries. The peaks and background of the diffraction pattern were modeled by using a pseudo-Voigt profile function and a shifted Chebyschev polynomial function, respectively. Initially background parameters along with the scale were refined and unit cell parameters, half-width (U, V and W) and mixing (Z) parameters of pseudo-Voigt function and peak asymmetry corrections were added in the subsequent refinement cycles.
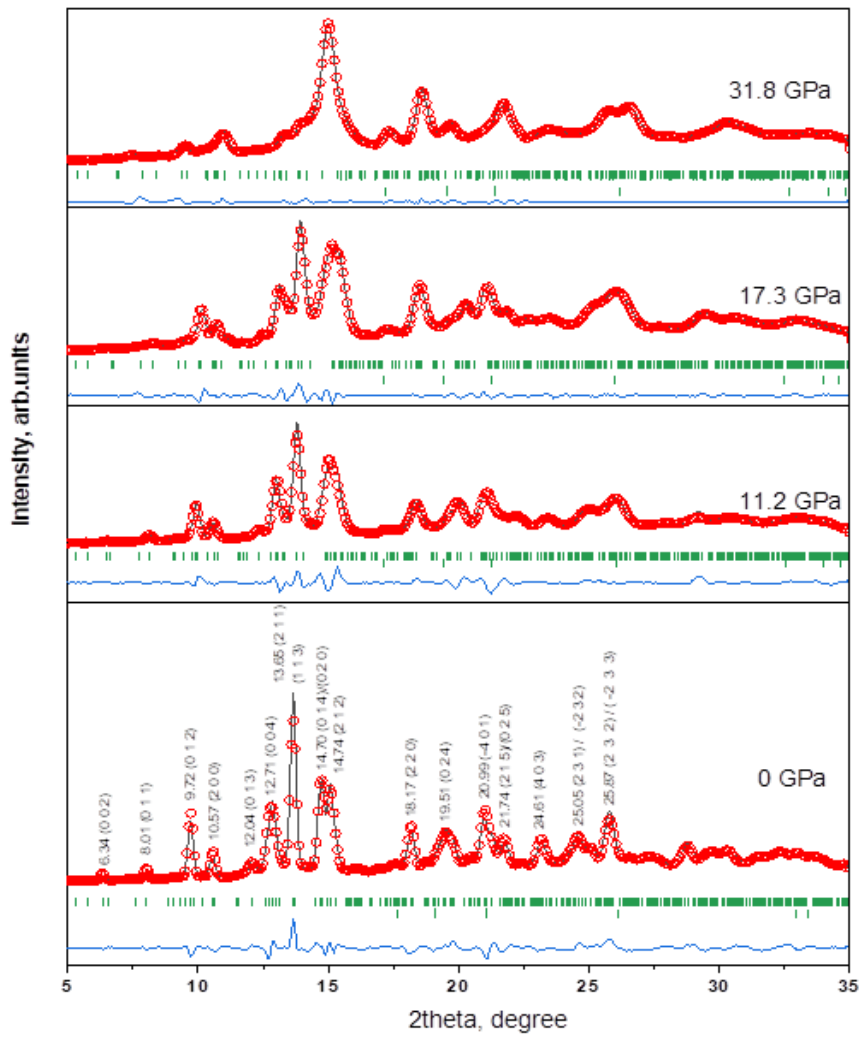
Figure 3. X-ray diffraction pattern of LTO for different pressures
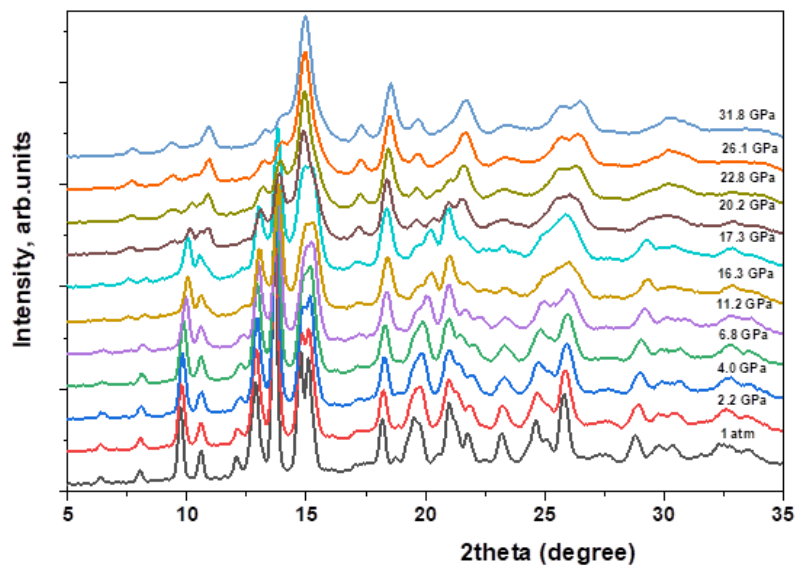

Figure 4. The phase generation of LTO in pressure medium

In Figure 4 all the intense peaks of LTO could be explained by any of the considered models. However, the intensities of weak peaks generation at high pressures are the sign of monoclinic P2 structures compared to the orthorhombic Cmc2$_1$ or Cmcm structures. The refinement of the position coordinates of all the possible models was subsequently carried out to further ascertain the structure of LTO. The goodness of fit was monitored from the residual (R-values) of refinements and differences between the observed and calculated diffraction patterns. The refinements with this monoclinic super-structure model indicate closely similar residuals while the unit cell parameter is doubled along the c-axis. Despite the structure consisting of twice the number of atoms in the asymmetric unit and having a larger unit cell, no better residuals as well as profile could be obtained in the super-structure model of monoclinic P2$_1$ structure. The P2 symmetry has smaller unit cell parameters and should exhibit extra reflections as well as detectable intensities. By the increasing of the pressure we observed some additional peaks, which is indicate that, it is possible to say for high pressure phase is related P2$_1$ (4) monoclinic and P2 (3) monoclinic transition. For the indication of phase transition, focused we on continuity of cell parameters and volume depends on pressure. Figure 5 demonstrates the non-linear progression of mentioned parameters.
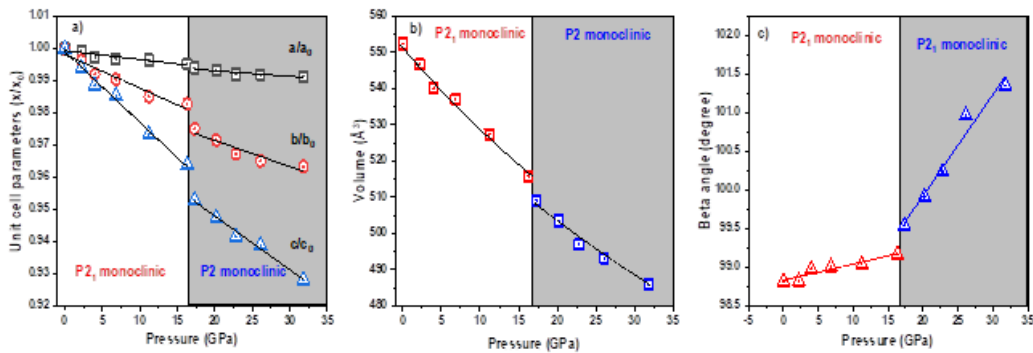

Figure 5. Pressure effect on unit cell parameters (a), volume (b) and beta angle (c) of LTO

There is not significant change at β-angle at pressures below 16.3 GPa. At higher pressures, it increases gradually (Figure 5c). The change in cell volume with increasing pressure is shown in Figure 5b which is calculated with Birch – Murnagan equation. The effect of pressure seen mostly from 16.3GPa to 22.8GPa range. The peaks between ~ 5 θ^0 to ~ 17 θ^0 are the fingerprint of monoclinic phase.

In Figure 3 at the first sight, it is clearly obvious that the (002), (011), (024), (215) / (025) peaks lost their intensities. As well as, the (231) / (-232) peak we lost at high pressure. The interval between ~14 θ^0 and ~16 θ^0 observed singlet (014) / (020) and (212) peaks merge during increasing pressure. The peak (200) seen ~10.58 θ^0 which turn to (-201) by the effect of pressure and we relate this by the shifting of "La" layers in monoclinic cell. This is the evidence of interlayer shifting to be nonstructural transition at low pressures. To determine structural changes the pressure was increased up to 30GPa.

The obtained structure analyzed with P2 monoclinic phase and seen that new phase appear in monoclinic phase. By the increasing of pressure to 17.3 GPa P2 phase become clear and more specific. The region between ~16.5 θ^0 and ~27.3 θ^0 shows highly relation with P2 phase. P2$_1$ space group for LTO. By the increasing of pressure as an expected

we observed some new peaks, mergers of peaks (particularly between ∼ 23 θ^0 to ∼ 27 θ^0). By the inducing high pressure, the peak positions and intensities turn to new unknown form. Raman and X-Ray analysis confirms this new form expected highly with P2 monoclinic structure.

Depend on titanium source at synthesis procedure it is also possible to see Pna2$_1$ (orthorhombic) phase. For instance, if the titanium source is tetrabutyl titanate we can see Pna2$_1$ (orthorhombic) phase-transition during high temperature (850^{0}C) (Lichtenberg *et al*., 2001) or high pressure (17.3 GPa) analysis of crystal structure instead of titanium isoproxide.

2.3. Raman Spectroscopy

Raman spectroscopic analysis made by LabRam Evolution at room temperature with the DAC from 1atm to 30Gpa, a small ruby crystal placed in the vicinity of the sample. Raman modes being sensitive to the variation of local coordination and distortion as well as to symmetry, the analyses of temperature dependent Raman mode can provide clear information on these features. Under ambient conditions, La$_2$Ti$_2$O$_7$ has monoclinic structure with space group P2$_1$. Low pressure Raman modes as expected as are indicate monoclinic (space group: P2$_1$) perovskite-like LTO structure (Li *et al*., 2008), which is share same structure with other rare-earth titan oxides as Pr$_2$Ti$_2$O$_7$ and Nd$_2$Ti$_2$O$_7$. From the theory the LTO possess to 132 (3n) normal modes of vibrations and 129 (3n-3) optical modes. Raman active modes the optic modes obey to Γ_{optic} =65A+64B and acoustic modes $\Gamma_{acoustic}$ = A + 2B (Sivagnanapalani *et al*., 2021). The spectrum divided sections for detailed analysis. Figure 7a shows low frequency region from 40 cm^{-1} to 460 cm^{-1}. It is confirmed from literature that, low frequency modes are highly related with RE – O (RE = La) vibrations, In the other hand, at Figure 7b high frequency modes from 460 cm^{-1} to 580 cm^{-1} regions are attributed to vibration of TiO$_6$ distorted octahedrons. The stretch related modes of Ti - O observed from 760 cm^{-1} to 850 cm^{-1} for LTO. Note that individual Raman lines (41 cm^{-1} - 138 cm^{-1}) are very narrow with as low FWHM as 5 cm^{-1}. This indicates rather a high structural quality of LTO powder sample synthesized by long-time solid state synthesis (Herrera *et al*., 2014).
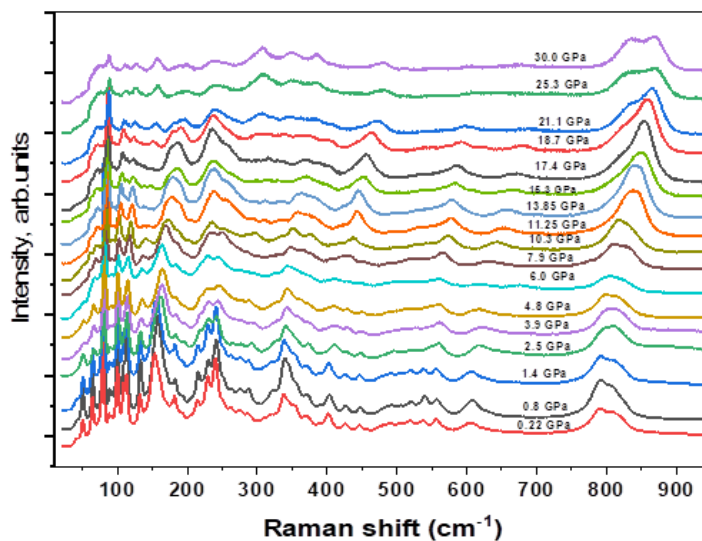

Figure 6. Raman vibrational spectra of LTO at elevated pressures

Raman spectrum recorded for LTO crystals is shown in Figure 6. The general profile of the spectrum resembles that one earlier reported for LTO, but the line frequency positions are noticeably different. In Raman spectra there are some peaks confirms phase transition between $P2_1$ (monoclinic) and $P2$ (monoclinic) phases. In La-O vibration related region peaks (228 cm^{-1}, 240 cm^{-1}, 351 cm^{-1}, 371 cm^{-1}, 426 cm^{-1}) follow linear shifting character up to 17.3 GPa as expected as, however anomalies start when pressure rise up and linearity of shifting changes to new form which is indicate new phenomenon. It is related to convergence of La and O atoms and bond length decreasing (Kim *et al*., 2003). In addition, peaks at TiO_6 distortion region (504 cm^{-1}, 519 cm^{-1}, 556 cm^{-1}) also show that, tilting and O_{II}–Ti–O_I bond angle deformation of octahedrons happen. The line at 504 cm^{-1} E_g - bending would be due to outer vibrations of TiO_6 octahedrons. Ti-O stretch related absorption line at 606 cm^{-1}, 794 cm^{-1}, 805 cm^{-1} are also demonstrates non-linear shifting from 17.3 GPa. The high-frequency line up of twin peaks at 794 and 805 cm^{-1} are assigned to the stretching mode of Ti-O vibrations Most interesting part observed at 794 cm^{-1}, 805 cm^{-1} Raman peaks, so when the pressure reach 8 GPa this peaks merge and split around 17 GPa.
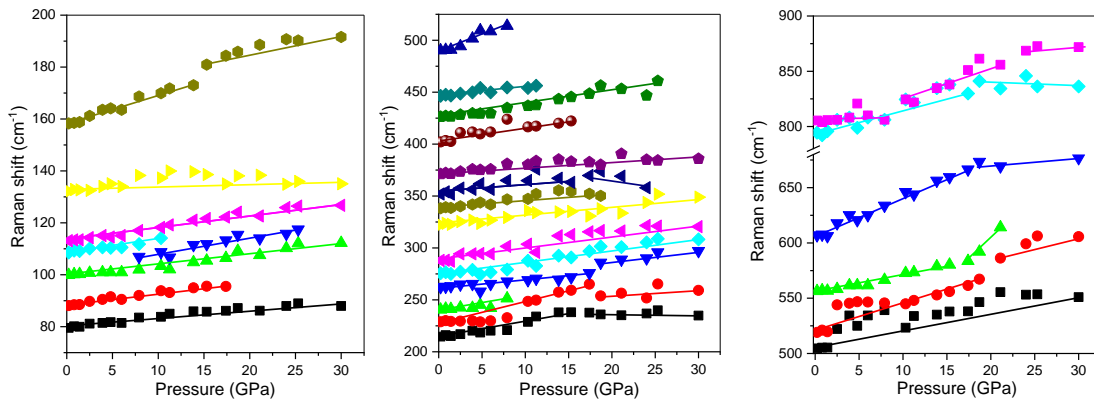

Figure 7. Raman modes shifting of LTO at elevated pressures

This phenomenon can be explained as Ti and O atoms bond length in octahedrons try to reach equilibrium distance (Kesari *et al*., 2016). For the low pressure oblast (below 5 GPa) the not phase related transition also observed. Figure 7 shows Raman shifts of LTO Raman peaks due to increasing of the pressure.

3. Conclusions

The $La_2Ti_2O_7$ structure was analyzed by XRD, Neutron diffraction and Raman spectroscopy. XRD and Raman spectroscopy measurement methods confirms that structure is $P2_1$ monoclinic at ambient condition by the pressure induced measurements it become obvious that structure turn to $P2$ monoclinic phase when pressure reach to 17.3GPa. This phase transition happen by shifting of "La" slabs, distortion of unit cell and the tilting of TiO_6 octohedrons.

Acknowledgments

References

Alanis, J., Ojeda-Galván, H.J., Rodríguez-Aranda, M.C., Rodríguez, A.G., Moreno García, H., Íñiguez, J. & Navarro-Contreras, H.R. (2019). High-pressure structural change in the ferroelectric layered perovskite Sr$_2$Nb$_2$O$_7$. *Physical Review B*, *100*(5), 054110. https://doi.org/10.1103/PhysRevB.100.054110

Gao, Z., Liu, Y., Lu, C., Ma, Y., Xia, Y., Fang, L. & He, D. (2017). Origin of the phase change from pyrochlore to perovskite-like layered structure and a new lead free ferroelectric. *arXiv preprint arXiv:1703.01016*. https://arxiv.org/abs/1703.01016

Gao, Z.P., Yan, H.X., Ning, H.P. & Reece, M.J. (2013). Ferroelectricity of Pr$_2$Ti$_2$O$_7$ ceramics with super high Curie point. *Advances in Applied Ceramics*, *112*(2), 69-74. https://doi.org/10.1179/1743676112Y.0000000030

Herrera, G., Jiménez-Mier, J. & Chavira, E. (2014). Layered-structural monoclinic–orthorhombic perovskite La$_2$Ti$_2$O$_7$ to orthorhombic LaTiO$_3$ phase transition and their microstructure characterization. *Materials Characterization*, 89, 13-22. https://doi.org/10.1016/j.matchar.2013.12.013

Hwang, D.W., Lee, J.S., Li, W. & Oh, S.H. (2003). Electronic band structure and photocatalytic activity of Ln$_2$Ti$_2$O$_7$ (Ln= La, Pr, Nd). *The Journal of Physical Chemistry B*, *107*(21), 4963-4970. https://doi.org/10.1021/jp034229n

Ishizawa, N., Marumo, F., Iwai, S., Kimura, M. & Kawamura, T. (1982). Compounds with perovskite-type slabs. V. A high-temperature modification of La$_2$Ti$_2$O$_7$. *Acta Crystallographica Section B: Structural Crystallography and Crystal Chemistry*, *38*(2), 368-372. https://doi.org/10.1107/S0567740882002994

Kesari, S., Salke, N.P., Patwe, S.J., Achary, S.N., Sinha, A.K., Sastry, P.U. & Rao, R. (2016). Structural stability and anharmonicity of Pr$_2$Ti$_2$O$_7$: Raman spectroscopic and XRD studies. *Inorganic Chemistry*, *55*(22), 11791-11800. https://doi.org/10.1021/acs.inorgchem.6b01873

Kim, H.G., Hwang, D.W., Bae, S.W., Jung, J.H. & Lee, J.S. (2003). Photocatalytic water splitting over La$_2$Ti$_2$O$_7$ synthesized by the polymerizable complex method. *Catalysis Letters*, 91, 193-198. https://doi.org/10.1023/B:CATL.0000007154.30343.23

Kozlenko, D., Kichanov, S., Lukin, E. & Savenko, B. (2018). The DN-6 neutron diffractometer for high-pressure research at half a megabar scale. *Crystals*, *8*(8), 331. https://doi.org/10.3390/cryst8080331

Li, Z., Chen, G., Tian, X. & Li, Y. (2008). Photocatalytic property of La$_2$Ti$_2$O$_7$ synthesized by the mineralization polymerizable complex method. *Materials Research Bulletin*, *43*(7), 1781-1788. https://doi.org/10.1016/j.materresbull.2007.07.010

Lichtenberg, F., Herrnberger, A., Wiedenmann, K. & Mannhart, J. (2001). Synthesis of perovskite-related layered A$_n$B$_n$O$_{3n+2}$= ABO$_X$ type niobates and titanates and study of their structural, electric and magnetic properties. *Progress in Solid State Chemistry*, *29*(1-2), 1-70. https://doi.org/10.1016/S0079-6786(01)00002-4

López-Pérez, J., Íñiguez, J. (2011). Ab initio study of proper topological ferroelectricity in layered perovskite La$_2$Ti$_2$O$_7$. *Physical Review B*, *84*(7), 075121. https://doi.org/10.1103/PhysRevB.84.075121

Mirzayev, M.N. (2020). Simultaneous measurements of heat flow rate and thermal properties of nano boron trioxide under neutron irradiation at the low and high temperature. *Vacuum*, 173, 109162. https://doi.org/10.1016/j.vacuum.2019.109162

Mirzayev, M.N., Mehdiyeva, R.N., Melikova, S.Z., Jabarov, S.H., Thabethe, T.T., Biira, S. & Tiep, N.V. (2019). Formation of color centers and concentration of defects in boron carbide irradiated at low gamma radiation doses. *Journal of the Korean Physical Society*, 74, 363-367. https://doi.org/10.3938/jkps.74.363

Mirzayev, M.N., Popov, E., Demir, E., Abdurakhimov, B.A., Mirzayeva, D.M., Sukratov, V.A. & Kristavchuk, O. (2020). Thermophysical behavior of boron nitride and boron trioxide

ceramics compounds with high energy electron fluence and swift heavy ion irradiated. *Journal of Alloys and Compounds*, 834, 155119. https://doi.org/10.1016/j.jallcom.2020.155119

Nanamatsu, S., Kimura, M., Doi, K., Matsushita, S. & Yamada, N. (1974). A new ferroelectric: $La_2Ti_2O_7$. *Ferroelectrics*, *8*(1), 511-513. https://doi.org/10.1080/00150197408234143

Patwe, S.J., Katari, V., Salke, N.P., Deshpande, S.K., Rao, R., Gupta, M.K. & Tyagi, A.K. (2015). Structural and electrical properties of layered perovskite type $Pr_2Ti_2O_7$: Experimental and theoretical investigations. *Journal of Materials Chemistry C*, *3*(17), 4570-4584. https://doi.org/10.1039/C5TC00242G

Schmalle, H.W., Williams, T., Reller, A., Linden, A. & Bednorz, J.G. (1993). The twin structure of $La_2Ti_2O_7$: X-Ray and transmission electron microscopy studies. *Acta Crystallographica Section B: Structural Science*, *49*(2), 235-244. https://doi.org/10.1107/S010876819200987X

Sivagnanapalani, P., Ansari, N.I. & Panda, P.K. (2021). $Nd_2Ti_2O_7$ (NTO) with high curie temperature (TC) for high temperature sensor applications. *Sensors International*, 2, 100093. https://doi.org/10.1016/j.sintl.2021.100093

Wang, J.W., Lang, M. & Zhang, J.M. (2010). Pressure-induced structural transformations in lanthanide titanates: La_2TiO_5 and Nd_2TiO_5. *Journal of Solid State Chemistry*, *183*(11). https://doi.org/10.1016/j.jssc.2010.09.014

Wang, X., Zhou, Q., Li, F., Wu, C., Gong, M., He, S. & Cui, T. (2022). Thermally enhanced piezoelectricity via the superstructure in $Ca_2Nb_2O_7$ single-crystals with ultra-high Curie temperature. *Journal of Materials Chemistry A*, *10*(38), 20473-20481. https://doi.org/10.1039/D2TA03412C

Yamamoto, N., Yagi, K., Honjo, G., Kimura, M. & Kawamura, T. (1980). New phases of $Sr_2Ta_2O_7$ and $Sr_2Nb_2O_7$ found by electron microscopy and diffraction. *Journal of the Physical Society of Japan*, *48*(1), 185-191. https://doi.org/10.1143/JPSJ.48.185

Yan, H., Ning, H., Kan, Y., Wang, P. & Reece, M.J. (2009). Piezoelectric ceramics with super-high curie points. *Journal of the American Ceramic Society*, *92*(10), 2270-2275. https://doi.org/10.1111/j.1551-2916.2009.03209.x

Zhang, F.X., Lian, J., Becker, U., Ewing, R.C., Wang, L.M., Hu, J. & Saxena, S.K. (2007). Structural change of layered perovskite $La_2Ti_2O_7$ at high pressures. *Journal of Solid State Chemistry*, *180*(2), 571-576. https://doi.org/10.1016/j.jssc.2006.11.022